

¹ **Critical transitions and the fragmenting of global forests**

² **Leonardo A. Saravia^{1 3}, Santiago R. Doyle¹, Benjamin Bond-Lamberty²**

³ 1. Instituto de Ciencias, Universidad Nacional de General Sarmiento, J.M. Gutierrez 1159 (1613), Los
⁴ Polvorines, Buenos Aires, Argentina.

⁵ 2. Pacific Northwest National Laboratory, Joint Global Change Research Institute at the University of
⁶ Maryland–College Park, 5825 University Research Court #3500, College Park, MD 20740, USA

⁷ 3. Corresponding author e-mail: lsaravia@ungs.edu.ar

⁸ **keywords:** Forest fragmentation, early warning signals, percolation, power-laws, MODIS, critical transitions

⁹ **Running title:** Critical fragmentation in global forest

¹⁰ **Abstract**

¹¹ 1. Forests provide critical habitat for many species, essential ecosystem services, and are coupled to
¹² atmospheric dynamics through exchanges of energy, water and gases. One of the most important
¹³ changes produced in the biosphere is the replacement of forest areas with human dominated landscapes.
¹⁴ This usually leads to fragmentation, altering the sizes of patches, the structure and function of the
¹⁵ forest. Here we studied the distribution and dynamics of forest patch sizes at a global level, examining
¹⁶ signals of a critical transition from an unfragmented to a fragmented state.

¹⁷ 2. We used MODIS vegetation continuous field to estimate the forest patches at a global level and defined
¹⁸ wide regions of connected forest across continents and big islands. We search for critical phase transi-
¹⁹ tions, where the system state of the forest changes suddenly at a critical point; this implies an abrupt
²⁰ change in connectivity that causes an increased fragmentation level. We studied the distribution of for-
²¹ est patch sizes and the dynamics of the largest patch over the last fourteen years. The conditions that
²² indicate that a region is near a critical fragmentation threshold are related to patch size distribution
²³ and temporal fluctuations of the largest patch.

²⁴ 3. We found some evidence that allows us to analyze fragmentation as a critical transition: most regions
²⁵ followed a power-law distribution. We also found that the Philippines region probably went through
²⁶ a critical transition from a fragmented to an unfragmented state. Then using the all the proposed
²⁷ conditions, only the tropical forest of Africa and South America met the criteria to be near a critical
²⁸ fragmentation threshold.

²⁹ 4. This implies that human pressures and climate forcings might trigger undesired effects of fragmentation,
³⁰ such as species loss and degradation of ecosystems services, in these regions. The simple criteria
³¹ proposed here could be used as an early warning to estimate the distance to a fragmentation threshold
³² in forest around the globe and could be used as a predictor of a planetary tipping point.

33 Introduction

34 Forests are one of the most important ecosystems on earth, providing habitat for a large proportion of species
35 and contributing extensively to global biodiversity (Crowther *et al.* 2015). In the previous century human
36 activities have influenced global bio-geochemical cycles (Bonan 2008; Canfield, Glazer & Falkowski 2010),
37 with one of the most dramatic changes being the replacement of 40% of Earth's formerly biodiverse land
38 areas with landscapes that contain only a few species of crop plants, domestic animals and humans (Foley
39 *et al.* 2011). These local changes have accumulated over time and now constitute a global forcing (Barnosky
40 *et al.* 2012).

41 Another global scale forcing that is tied to habitat destruction is fragmentation, which is defined as the
42 division of a continuous habitat into separated portions that are smaller and more isolated. Fragmentation
43 produces multiple interwoven effects: reductions of biodiversity between 13% and 75%, decreasing forest
44 biomass, and changes in nutrient cycling (Haddad *et al.* 2015). The effects of fragmentation are not only
45 important from an ecological point of view but also that of human activities, as ecosystem services are deeply
46 influenced by the level of landscape fragmentation (Mitchell *et al.* 2015).

47 Ecosystems have complex interactions between species and present feedbacks at different levels of organiza-
48 tion (Gilman *et al.* 2010), and external forcings can produce abrupt changes from one state to another,
49 called critical transitions (Scheffer *et al.* 2009). These abrupt state shifts cannot be linearly forecasted from
50 past changes, and are thus difficult to predict and manage (Scheffer *et al.* 2009). Critical transitions have
51 been detected mostly at local scales (Drake & Griffen 2010; Carpenter *et al.* 2011), but the accumulation of
52 changes in local communities that overlap geographically can propagate and theoretically cause an abrupt
53 change of the entire system at larger scales (Barnosky *et al.* 2012). Coupled with the existence of global
54 scale forcings, this implies the possibility that a critical transition could occur at a global scale (Rockstrom
55 *et al.* 2009; Folke *et al.* 2011).

56 Complex systems can experience two general classes of critical transitions (Solé 2011). In so-called first
57 order transitions, a catastrophic regime shift that is mostly irreversible occurs because of the existence of
58 alternative stable states (Scheffer *et al.* 2001). This class of transitions is suspected to be present in a variety
59 of ecosystems such as lakes, woodlands, coral reefs (Scheffer *et al.* 2001), semi-arid grasslands (Bestelmeyer
60 *et al.* 2011), and fish populations (Vasilakopoulos & Marshall 2015). They can be the result of positive
61 feedback mechanisms (Martín *et al.* 2015); for example, fires in some forest ecosystems were more likely to
62 occur in previously burned areas than in unburned places (Kitzberger *et al.* 2012).

63 The other class of critical transitions are continuous or second order transitions (Solé & Bascompte 2006).

64 In these cases, there is a narrow region where the system suddenly changes from one domain to another,
65 with the change being continuous and in theory reversible. This kind of transitions were suggested to be
66 present in tropical forest (Pueyo *et al.* 2010), semi-arid mountain ecosystems (McKenzie & Kennedy 2012),
67 tundra shrublands (Naito & Cairns 2015). The transition happens at critical point where we can observe a
68 distinctive spatial pattern: scale invariant fractal structures characterized by power law patch distributions
69 (Stauffer & Aharony 1994).

70 There are several processes that can convert a catastrophic transition to a second order transitions (Martín
71 *et al.* 2015). These include stochasticity, such as demographic fluctuations, spatial heterogeneities, and/or
72 dispersal limitation. All these components are present in forest around the globe (Seidler & Plotkin 2006;
73 Filotas *et al.* 2014; Fung *et al.* 2016), thus continuous transitions might be more probable than catastrophic
74 transitions. Moreover there is some evidence of recovery in some systems that supposedly suffered an
75 irreversible transition produced by overgrazing (Zhang *et al.* 2005) and desertification (Allington & Valone
76 2010).

77 The spatial phenomena observed in continuous critical transitions deal with connectivity, a fundamental
78 property of general systems and ecosystems from forests (Ochoa-Quintero *et al.* 2015) to marine ecosystems
79 (Leibold & Norberg 2004) and the whole biosphere (Lenton & Williams 2013). When a system goes from a
80 fragmented to a connected state we say that it percolates (Solé 2011). Percolation implies that there is a
81 path of connections that involves the whole system. Thus we can characterize two domains or phases: one
82 dominated by short-range interactions where information cannot spread, and another in which long range
83 interactions are possible and information can spread over the whole area. (The term “information” is used
84 in a broad sense and can represent species dispersal or movement.)

85 Thus, there is a critical “percolation threshold” between the two phases, and the system could be driven
86 close to or beyond this point by an external force; climate change and deforestation are the main forces
87 that could be the drivers of such a phase change in contemporary forests (Bonan 2008; Haddad *et al.* 2015).
88 There are several applications of this concept in ecology: species’ dispersal strategies are influenced by
89 percolation thresholds in three-dimensional forest structure (Solé, Bartumeus & Gamarra 2005), and it has
90 been shown that species distributions also have percolation thresholds (He & Hubbell 2003). This implies
91 that pushing the system below the percolation threshold could produce a biodiversity collapse (Bascompte
92 & Solé 1996; Solé, Alonso & Saldaña 2004; Pardini *et al.* 2010); conversely, being in a connected state (above
93 the threshold) could accelerate the invasion of forest into prairie (Loehle, Li & Sundell 1996; Naito & Cairns
94 2015).

95 One of the main challenges with systems that can experience critical transitions—of any kind—is that the

96 value of the critical threshold is not known in advance. In addition, because near the critical point a small
97 change can precipitate a state shift of the system, they are difficult to predict. Several methods have been
98 developed to detect if a system is close to the critical point, e.g. a deceleration in recovery from perturbations,
99 or an increase in variance in the spatial or temporal pattern (Hastings & Wysham 2010; Carpenter *et al.*
100 2011; Boettiger & Hastings 2012; Dai *et al.* 2012).

101 In this study, our objective is to look for evidence that forests around the globe are near continuous critical
102 point that represent a fragmentation threshold. We use the framework of percolation to first evaluate if
103 forest patch distribution at a continental scale is described by a power law distribution and then examined
104 the fluctuations of the largest patch. The advantage of using data at a continental scale is that for very large
105 systems the transitions are very sharp (Solé 2011) and thus much easier to detect than at smaller scales,
106 where noise can mask the signals of the transition.

107 Methods

108 Study areas definition

109 We analyzed mainland forests at a continental scale, covering the whole globe, by delimiting land areas with
110 a near-contiguous forest cover, separated with each other by large non-forested areas. Using this criterion,
111 we delimited the following forest regions. In America, three regions were defined: South America temperate
112 forest (SAT), subtropical and tropical forest up to Mexico (SAST), and USA and Canada forest (NA). Europe
113 and North Asia were treated as one region (EUAS). The rest of the delimited regions were South-east Asia
114 (SEAS), Africa (AF), and Australia (OC). We also included in the analysis islands larger than 10^5 km². The
115 mainland region has the number 1 e.g. OC1, and the nearby islands have consecutive numeration (Appendix
116 S4, figure S1-S6).

117 Forest patch distribution

118 We studied forest patch distribution in each defined area from 2000 to 2014 using the MODerate-resolution
119 Imaging Spectroradiometer (MODIS) Vegetation Continuous Fields (VCF) Tree Cover dataset version 051
120 (DiMiceli *et al.* 2015). This dataset is produced at a global level with a 231-m resolution, from 2000 onwards
121 on an annual basis. There are several definition of forest based on percent tree cover (Sexton *et al.* 2015),
122 we choose a 30% threshold to convert the percentage tree cover to a binary image of forest and non-forest
123 pixels. This was the definition used by the United Nations' International Geosphere-Biosphere Programme
124 (Belward 1996), and studies of global fragmentation (Haddad *et al.* 2015). This definition avoids the errors

125 produced by low discrimination of MODIS VCF between forest and dense herbaceous vegetation at low forest
126 cover (Sexton *et al.* 2015). Patches of contiguous forest were determined in the binary image by grouping
127 connected forest pixels using a neighborhood of 8 forest units (Moore neighborhood).

128 **Percolation theory**

129 A more in-depth introduction to percolation theory can be found elsewhere (Stauffer & Aharony 1994) and
130 a review from an ecological point of view is available (Oborny, Szabó & Meszéna 2007). Here, to explain
131 the basic elements of percolation theory we formulate a simple model: we represent our area of interest by a
132 square lattice and each site of the lattice can be occupied—e.g. by forest—with a probability p . The lattice
133 will be more occupied when p is greater, but the sites are randomly distributed. We are interested in the
134 connection between sites, so we define a neighborhood as the eight adjacent sites surrounding any particular
135 site. The sites that are neighbors of other occupied sites define a patch. When there is a patch that connects
136 the lattice from opposite sides, it is said that the system percolates. When p is increased from low values, a
137 percolating patch suddenly appears at some value of p called the critical point p_c .

138 Thus percolation is characterized by two well defined phases: the unconnected phase when $p < p_c$ (called
139 subcritical in physics), in which species cannot travel far inside the forest, as it is fragmented; in a general
140 sense, information cannot spread. The second is the connected phase when $p > p_c$ (supercritical), species
141 can move inside a forest patch from side to side of the area (lattice), i.e. information can spread over the
142 whole area. Near the critical point several scaling laws arise: the structure of the patch that spans the area
143 is fractal, the size distribution of the patches is power-law, and other quantities also follow power-law scaling
144 (Stauffer & Aharony 1994).

145 The value of the critical point p_c depends on the geometry of the lattice and on the definition of the
146 neighborhood, but other power-law exponents only depend on the lattice dimension. Close to the critical
147 point, the distribution of patch sizes is:

148 (1) $n_s(p_c) \propto s^{-\alpha}$

149 where $n_s(p)$ is the number of patches of size s . The exponent α does not depend on the details of the
150 model and it is called universal (Stauffer & Aharony 1994). These scaling laws can be applied for landscape
151 structures that are approximately random, or at least only correlated over short distances (Gastner *et al.*
152 2009). In physics this is called “isotropic percolation universality class”, and corresponds to an exponent
153 $\alpha = 2.05495$. If we observe that the patch size distribution has another exponent it will not belong to this
154 universality class and some other mechanism should be invoked to explain it. Percolation thresholds can also

155 be generated by models that have some kind of memory (Hinrichsen 2000; Ódor 2004): for example, a patch
156 that has been exploited for many years will recover differently than a recently deforested forest patch. In
157 this case, the system could belong to a different universality class, or in some cases there is no universality,
158 in which case the value of α will depend on the parameters and details of the model (Corrado, Cherubini &
159 Pennetta 2014).

160 To illustrate these concepts, we conducted simulations with a simple forest model with only two states:
161 forest and non-forest. This type of model is called a “contact process” and was introduced for epidemics
162 (Harris 1974), but has many applications in ecology (Solé & Bascompte 2006; Gastner *et al.* 2009). A site
163 with forest can become extinct with probability e , and produce another forest site in a neighborhood with
164 probability c . We use a neighborhood defined by an isotropic power law probability distribution. We defined
165 a single control parameter as $\lambda = c/e$ and ran simulations for the subcritical fragmentation state $\lambda < \lambda_c$,
166 with $\lambda = 2$, near the critical point for $\lambda = 2.5$, and for the supercritical state with $\lambda = 5$ (see Appendix S2,
167 gif animations).

168 Patch size distributions

169 We fitted the empirical distribution of forest patch areas, based on the MODIS-derived data described above,
170 to four distributions using maximum likelihood estimation (Goldstein, Morris & Yen 2004; Clauset, Shalizi
171 & Newman 2009). The distributions were: power-law, power-law with exponential cut-off, log-normal, and
172 exponential. We assumed that the patch size distribution is a continuous variable that was discretized by
173 remote sensing data acquisition procedure.

174 We set a minimal patch size (X_{min}) at nine pixels to fit the patch size distributions to avoid artifacts at patch
175 edges due to discretization (Weerman *et al.* 2012). Besides this hard X_{min} limit we set due to discretization,
176 the power-law distribution needs a lower bound for its scaling behavior. This lower bound is also estimated
177 from the data by maximizing the Kolmogorov-Smirnov (KS) statistic, computed by comparing the empirical
178 and fitted cumulative distribution functions (Clauset *et al.* 2009). We also calculated the uncertainty of the
179 parameters using a non-parametric bootstrap method (Efron & Tibshirani 1994), and computed corrected
180 Akaike Information Criteria (AIC_c) and Akaike weights for each model (Burnham & Anderson 2002). Akaike
181 weights (w_i) are the weight of evidence in favor of model i being the actual best model given that one of the
182 N models must be the best model for that set of N models.

183 Additionally, we computed the goodness of fit of the power-law model following the bootstrap approach
184 described by Clauset et. al (2009), where simulated data sets following the fitted model are generated, and a

185 p -value computed as the proportion of simulated data sets that has a KS statistic less extreme than empirical
186 data. The criterion to reject the power law model suggested by Clauset et. al (2009) was $p \leq 0.1$, but as we
187 have a very large n , meaning that negligible small deviations could produce a rejection (Klaus, Yu & Plenz
188 2011), we chose a $p \leq 0.05$ to reject the power law model.

189 To test for differences between the fitted power law exponent for each study area we used a generalized least
190 squares linear model (Zuur *et al.* 2009) with weights and a residual auto-correlation structure. Weights were
191 the bootstrapped 95% confidence intervals and we added an auto-regressive model of order 1 to the residuals
192 to account for temporal autocorrelation.

193 Largest patch dynamics

194 The largest patch is the one that connects the highest number of sites in the area. This has been used
195 extensively to indicate fragmentation (Gardner & Urban 2007; Ochoa-Quintero *et al.* 2015). The relation of
196 the size of the largest patch S_{max} to critical transitions has been extensively studied in relation to percolation
197 phenomena (Stauffer & Aharony 1994; Bazant 2000; Botet & Ploszajczak 2004), but seldom used in ecological
198 studies (for an exception see Gastner *et al.* (2009)). When the system is in a connected state ($p > p_c$) the
199 landscape is almost insensitive to the loss of a small fraction of forest, but close to the critical point a minor
200 loss can have important effects (Solé & Bascompte 2006; Oborny *et al.* 2007), because at this point the
201 largest patch will have a filamentary structure, i.e. extended forest areas will be connected by thin threads.
202 Small losses can thus produce large fluctuations.

203 One way to evaluate the fragmentation of the forest is to calculate the proportion of the largest patch against
204 the total area (Keitt, Urban & Milne 1997). The total area of the regions we are considering (Appendix S4,
205 figures S1-S6) may not be the same than the total area that the forest could potentially occupy, thus a more
206 accurate way to evaluate the weight of S_{max} is to use the total forest area, that can be easily calculated
207 summing all the forest pixels. We calculate the proportion of the largest patch for each year, dividing S_{max}
208 by the total forest area of the same year: $RS_{max} = S_{max}/\sum_i S_i$. This has the effect of reducing the S_{max}
209 fluctuations produced due to environmental or climatic changes influences in total forest area. When the
210 proportion RS_{max} is large (more than 60%) the largest patch contains most of the forest so there are fewer
211 small forest patches and the system is probably in a connected phase. Conversely, when it is low (less than
212 20%), the system is probably in a fragmented phase (Saravia & Momo 2017).

213 The RS_{max} is a useful qualitative index that does not tell us if the system is near or far from the critical
214 transition; this can be evaluated using the temporal fluctuations. We calculate the fluctuations around the

mean with the absolute values $\Delta S_{max} = S_{max}(t) - \langle S_{max} \rangle$, using the proportions of RS_{max} . To characterize fluctuations we fitted three empirical distributions: power-law, log-normal, and exponential, using the same methods described previously. We expect that large fluctuation near a critical point have heavy tails (log-normal or power-law) and that fluctuations far from a critical point have exponential tails, corresponding to Gaussian processes (Rooij *et al.* 2013). As the data set spans 15 years, we do not have enough power to reliably detect which distribution is better (Clauset *et al.* 2009). To improve this we performed the goodness of fit test described above for all the distributions. We generated animated maps showing the fluctuations of the two largest patches to aid in the interpretations of the results.

A robust way to detect if the system is near a critical transition is to analyze the increase in variance of the density (Benedetti-Cecchi *et al.* 2015). It has been demonstrated that the variance increase in density appears when the system is very close to the transition (Corrado *et al.* 2014), thus practically it does not constitute an early warning indicator. An alternative is to analyze the variance of the fluctuations of the largest patch ΔS_{max} : the maximum is attained at the critical point but a significant increase occurs well before the system reaches the critical point (Corrado *et al.* 2014). In addition, before the critical fragmentation, the skewness of the distribution of ΔS_{max} should be negative, implying that fluctuations below the average are more frequent. We characterized the increase in the variance using quantile regression: if variance is increasing the slopes of upper or/and lower quartiles should be positive or negative.

All statistical analyses were performed using the GNU R version 3.3.0 (R Core Team 2015), using code provided by Cosma R. Shalizi for fitting the power law with exponential cutoff model and the poweRlaw package (Gillespie 2015) for fitting the other distributions. For the generalized least squares linear model we used the R function gls from package nlme (Pinheiro *et al.* 2016); and we fitted quantile regressions using the R package quantreg (Koenker 2016). Image processing was done in MATLAB r2015b (The Mathworks Inc.). The complete source code for image processing and statistical analysis, and the patch size data files are available at figshare <http://dx.doi.org/10.6084/m9.figshare.4263905>.

Results

The figure 1 shows an example of the distribution of the biggest 200 patches for years 2000 and 2014, this distribution is highly variable, but the biggest patch usually maintains its place. Sometimes the biggest patch breaks and then big fluctuations in its size are observed, as we will analyze below. Smaller patches can merge or break more easily so they enter or leave the list of 200, and this is why there is a color change across years.

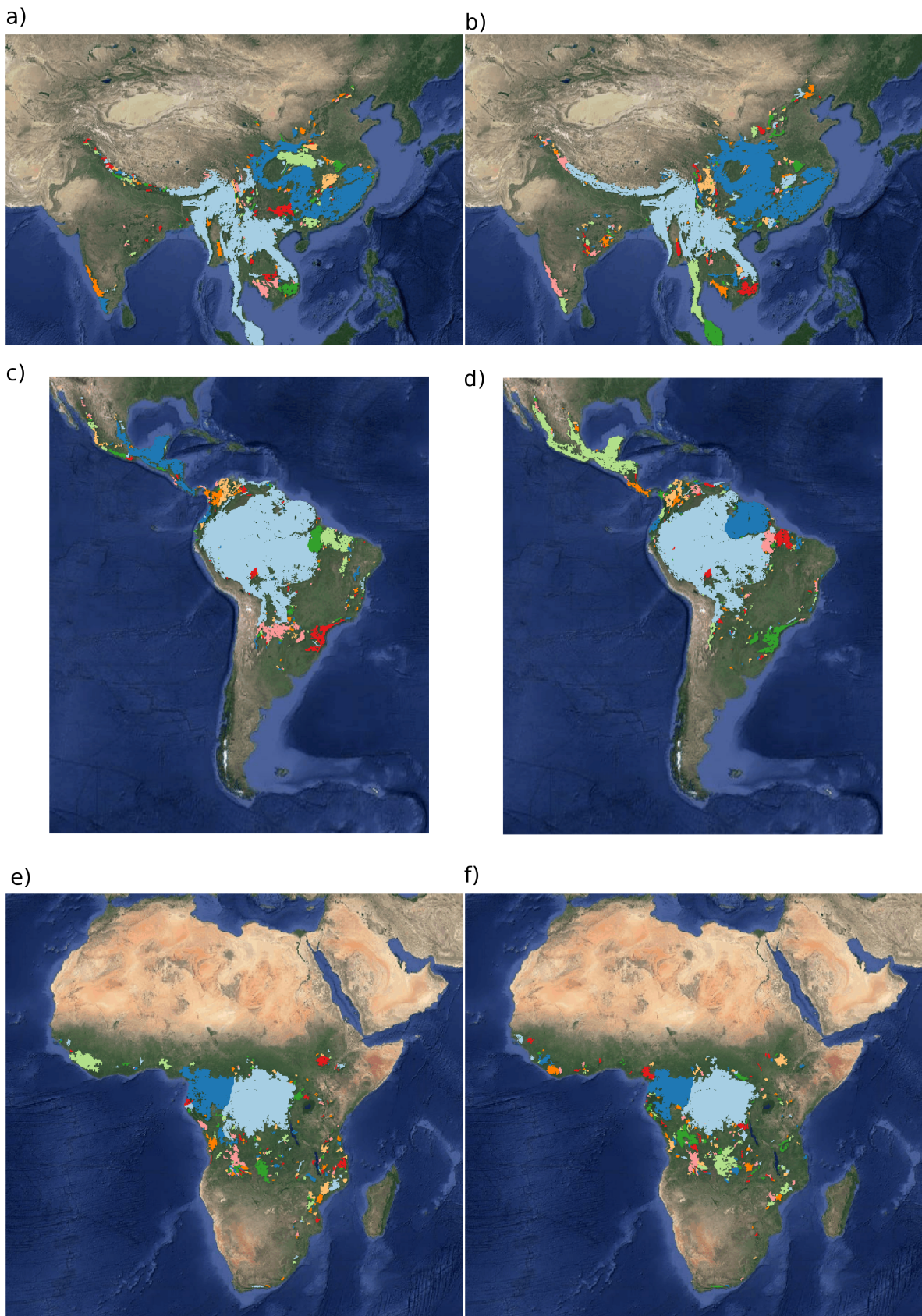


Figure 1: Forest patch distributions for continental regions for the years 2000 and 2014. The images are the 200 biggest patches, showed at a coarse pixel scale of 2.5 Km. The regions are: a) & b) southeast Asia; c) & d) South America subtropical and tropical and e) & f) Africa mainland, for the years 2000 and 2014 respectively.

245 The power law distribution was selected as the best model in 92% of the cases (Appendix S4, Figure S7).
246 In a small number of cases (1%) the power law with exponential cutoff was selected, but the value of the
247 parameter α was similar by ± 0.02 to the pure power law. Additionally the patch size where the exponential
248 tail begins is very large, thus we used the power law parameters for this cases (See Appendix S4, Figure S2,
249 region EUAS3). In finite-size systems the favored model should be the power law with exponential cutoff,
250 because the power-law tails are truncated to the size of the system (Stauffer & Aharony 1994). Here the
251 regions are so large that the cutoff is practically not observed.

252 There is only one region that did not follow a power law: Eurasia mainland, which showed a log-normal
253 distribution, representing 7% of the cases. The log-normal and power law are both heavy tailed distributions
254 and difficult to distinguish, but in this case Akaike weights have very high values for log-normal (near 1),
255 meaning that this is the only possible model. In addition, the goodness of fit tests clearly rejected the power
256 law model in all cases for this region (Appendix S4, table S1, region EUAS1). In general the goodness of fit
257 test rejected the power law model in fewer than 10% of cases. In large forest areas like Africa mainland (AF1)
258 or South America tropical-subtropical (SAST1), larger deviations are expected and the rejections rates are
259 higher so the proportion is 30% or less (Appendix S4, Table S1).

260 Taking into account the bootstrapped confidence intervals of each power law exponent (α) and the temporal
261 autocorrelation, there were no significant differences between α for the regions with the biggest (greater than
262 10^7 km^2) forest areas (Figure 2 and Appendix S4, Figure S8). There were also no differences between these
263 regions and smaller ones (Appendix S4, Tables S2 & S3), and all the slopes of α were not different from
264 0 (Appendix S4, Table S3). This implies a global average $\alpha = 1.908$, with a bootstrapped 95% confidence
265 interval between 1.898 and 1.920.

266 The proportion of the largest patch relative to total forest area RS_{max} for regions with more than 10^7 km^2
267 of forest is shown in figure 3. South America tropical and subtropical (SAST1) and North America (NA1)
268 have a higher RS_{max} of more than 60%, and other big regions 40% or less. For regions with less total
269 forest area (Appendix S4, figure S9 & Table 1), the United Kingdom (EUAS3) has a very low proportion
270 near 1%, while other regions such as New Guinea (OC2) and Malaysia/Kalimantan (OC3) have a very high
271 proportion. SEAS2 (Philippines) is a very interesting case because it seems to be under 30% until the year
272 2005, fluctuates in the range 30-60%, and then stays over 60% (Appendix S4, figure S9).

273 We analyzed the distributions of fluctuations of the largest patch relative to total forest area ΔRS_{max}
274 and the fluctuations of the largest patch ΔS_{max} . The model selection for ΔS_{max} resulted in power law
275 distributions for all regions (Appendix S4, table S6). For ΔRS_{max} instead some regions showed exponential
276 distributions: Eurasia mainland (EUAS1), New Guinea (OC2), Malaysia (OC3), New Zealand (OC6, OC8)

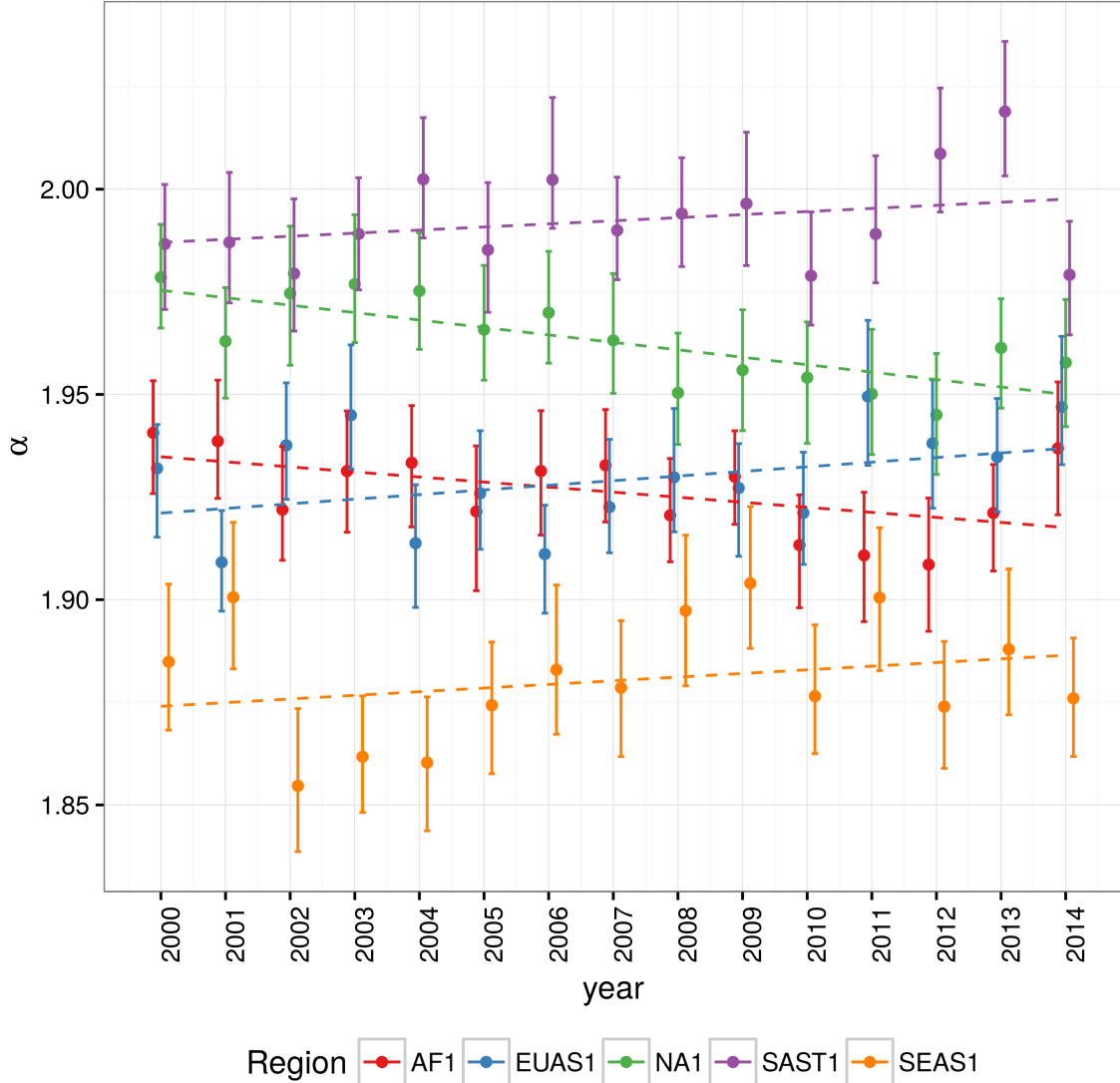


Figure 2: Power law exponents (α) of forest patch distributions for regions with total forest area $> 10^7 \text{ km}^2$. Dashed horizontal lines are the fitted generalized least squares linear model, with 95% confidence interval error bars estimated by bootstrap resampling. The regions are AF1: Africa mainland, EUAS1: Eurasia mainland, NA1: North America mainland, SAST1: South America subtropical and tropical, SEAS1: Southeast Asia mainland. For EUAS1 the best model is log-normal but the exponents are included here for comparison.

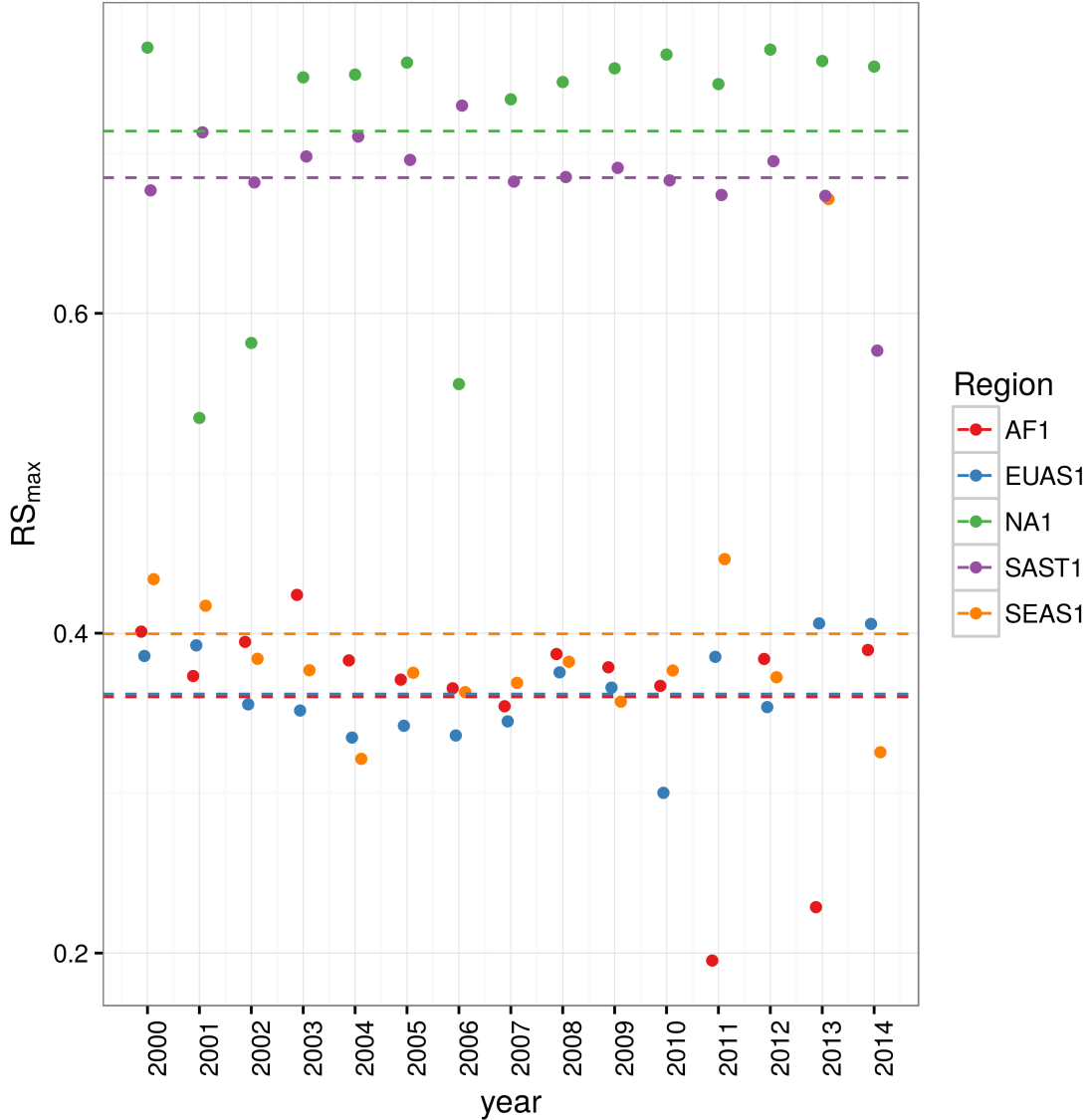


Figure 3: Largest patch proportion relative to total forest area RS_{max} , for regions with total forest area $> 10^7 \text{ km}^2$. Dashed lines are averages across time. The regions are AF1: Africa mainland, EUAS1: Eurasia mainland, NA1: North America mainland, SAST1: South America tropical and subtropical, SEAS1: Southeast Asia mainland.

277 and Java (OC7), all others were power laws (Appendix S4, Table S7). The goodness of fit test (GOF) did
278 not reject power laws in any case, but neither did it reject the other models except in a few cases; this was
279 due to the small number of observations. We only considered fluctuations to follow a power law when this
280 distribution was selected for both absolute and relative fluctuations.

281 The animations of the two largest patches (Appendix S3, largest patch gif animations) qualitatively shows
282 the nature of fluctuations and if the state of the forest is connected or not. If the largest patch is always
283 the same patch over time, the forest is probably not fragmented; this happens for regions with RS_{max} of
284 more than 40% such as AF2 (Madagascar), NA1 (North America), and OC3 (Malaysia). In the regions with
285 RS_{max} between 40% and 30% the identity of the largest patch could change or stay the same in time. For
286 OC7 (Java) the largest patch changes and for AF1 (Africa mainland) it stays the same. Only for EUAS1
287 (Eurasia mainland) we observed that the two largest patches are always the same, implying that this region
288 is probably composed of two independent domains and should be divided in further studies. The regions
289 with RS_{max} less than 25%: SAST2 (Cuba) and EUAS3 (United Kingdom), the largest patch always changes
290 reflecting their fragmented state. In the case of SEAS2 (Philippines) a transition is observed, with the
291 identity of the largest patch first variable, and then constant after 2010.

292 The results of quantile regressions are identical for ΔRS_{max} and ΔS_{max} (Appendix S4, table S4). Among the
293 biggest regions, Africa (AF1) has upper and lower quantiles with significantly negative slopes, but the lower
294 quantile slope is lower, implying that negative fluctuations and variance are increasing (Figure 4). Eurasia
295 mainland (EUAS1) has only the upper quantile significant with a positive slope, suggesting an increase in the
296 variance. North America mainland (NA1) exhibits a significant lower quantile with positive slope, implying
297 decreasing variance. Finally, for mainland Australia, all quantiles are significant, and the slope of the lower
298 quantiles is greater than the upper ones, showing that variance is decreasing (Appendix S4, figure S10).
299 These results are summarized in Table 1.

300 The conditions that indicate that a region is near a critical fragmentation threshold are that patch size
301 distributions follow a power law; temporal ΔRS_{max} fluctuations follow a power law; variance of ΔRS_{max} is
302 increasing in time; and skewness is negative. All these conditions were true only for Africa mainland (AF1)
303 and South America tropical & subtropical (SAST1).

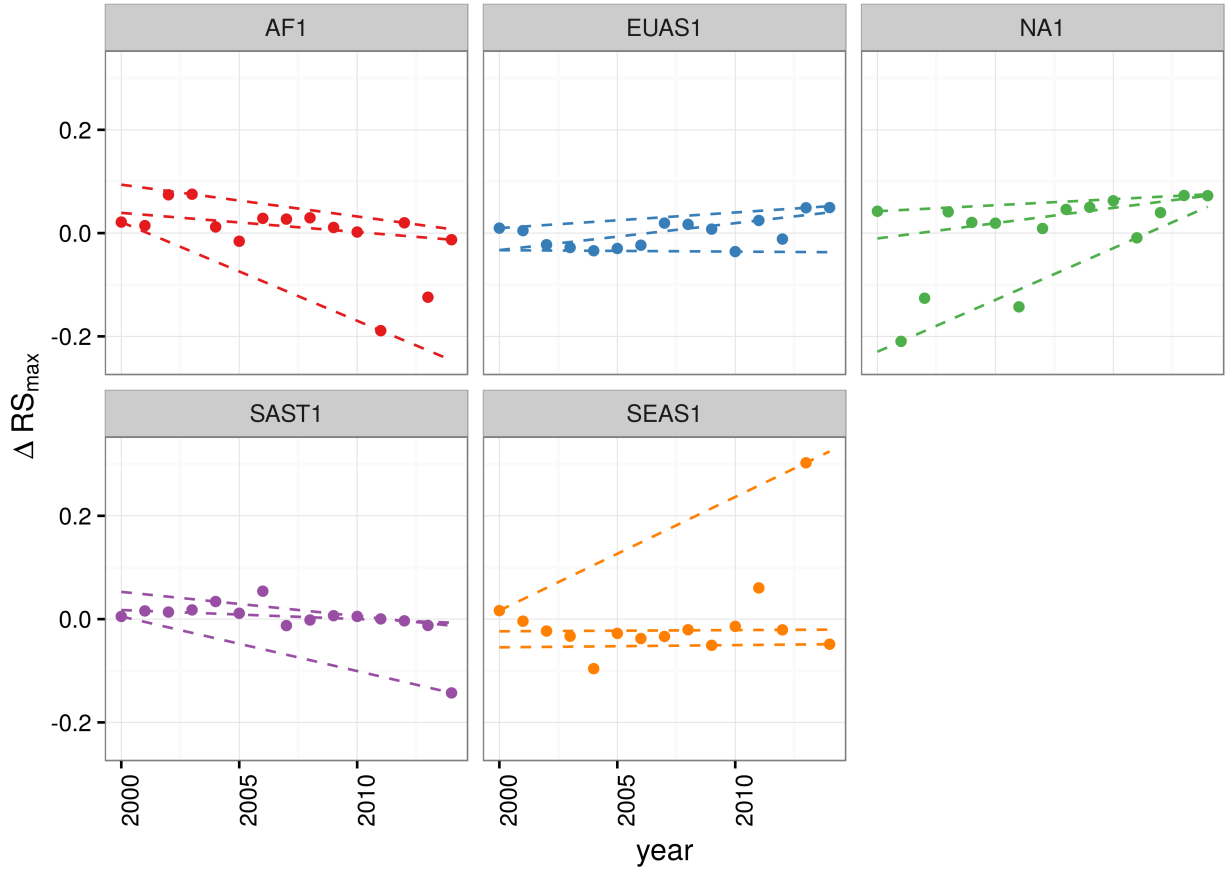


Figure 4: Largest patch fluctuations for regions with total forest area $> 10^7 \text{ km}^2$ across years. The patch sizes are relative to the total forest area of the same year. Dashed lines are 90%, 50% and 10% quantile regressions, to show if fluctuations were increasing. The regions are AF1: Africa mainland, EUAS1: Eurasia mainland, NA1: North America mainland, SAST1: South America tropical and subtropical, SEAS1: Southeast Asia mainland.

Table 1: Regions and indicators of closeness to a critical fragmentation threshold. Where, RS_{max} is the largest patch divided by the total forest area, ΔRS_{max} are the fluctuations of RS_{max} around the mean, skewness was calculated for RS_{max} and the increase or decrease in the variance was estimated using quantile regressions, NS means the results were non-significant. The conditions that determine the closeness to a threshold are: power law distributions in patch sizes and ΔRS_{max} ; increasing variance of ΔRS_{max} and negative skewness.

Region	Description	Average	Patch Size			
		RS_{max}	Distrib	ΔRS_{max}	Distrib.	Skewness
AF1	Africa mainland	0.36	Power	Power	-1.8630	Increase
AF2	Madagascar	0.65	Power	Power	-0.2478	NS
EUAS1	Eurasia, mainland	0.36	LogNormal	Exp	0.4016	Increase
EUAS2	Japan	0.94	Power	Power	0.0255	NS
EUAS3	United Kingdom	0.07	Power	Power	2.1330	NS
NA1	North America, mainland	0.71	Power	Power	-1.5690	Decrease
NA5	Newfoundland	0.87	Power	Power	-0.7411	NS
OC1	Australia, Mainland	0.28	Power	Power	0.0685	Decrease
OC2	New Guinea	0.97	Power	Exp	0.1321	Decrease
OC3	Malaysia/Kalimantan	0.97	Power	Exp	-0.9633	NS
OC4	Sumatra	0.92	Power	Power	1.3150	Increase
OC5	Sulawesi	0.87	Power	Power	-0.3863	NS
OC6	New Zealand South Island	0.76	Power	Exp	-0.6683	NS
OC7	Java	0.38	Power	Exp	-0.1948	NS
OC8	New Zealand North Island	0.75	Power	Exp	0.2940	NS
SAST1	South America, Tropical and subtropical forest up to Mexico	0.68	Power	Power	-2.7760	Increase
SAST2	Cuba	0.21	Power	Power	0.2751	NS
SAT1	South America, Temperate forest	0.60	Power	Power	-1.5070	Decrease
SEAS1	Southeast Asia, Mainland	0.40	Power	Power	3.0030	NS
SEAS2	Philippines	0.54	Power	Power	0.3113	Increase

304 Discussion

305 We found that the forest patch distribution of most regions of the world followed power laws spanning
 306 seven orders of magnitude. These include tropical rainforest, boreal and temperate forest. Power laws have
 307 previously been found for several kinds of vegetation, but never at global scales as in this study. Interestingly,
 308 Eurasia does not follow a power law, but it is a geographically extended region, consisting of different domains
 309 (as we observed in the largest patch animations, Appendix S2). It is known that the union of two independent
 310 power law distributions produces a lognormal distribution (Rooij *et al.* 2013). Future studies should split
 311 this region into two or more new regions, and test if the underlying distributions are power laws.
 312 Several mechanisms have been proposed for the emergence of power laws in forest: the first is related self
 313 organized criticality (SOC), when the system is driven by its internal dynamics to a critical state; this has

been suggested mainly for fire-driven forests (Zinck & Grimm 2009; Hantson, Pueyo & Chuvieco 2015). Real ecosystems do not seem to meet the requirements of SOC dynamics: their dynamics are influenced by external forces, and interactions are non-homogeneous (i.e. vary from place to place) (Sole, Alonso & Mckane 2002). Moreover, SOC requires a memory effect: fire scars in a site should accumulate and interfere with the propagation of a new fire. Pueyo et al. (2010) did not find such effect for tropical forests, and suggest that other mechanisms might produce the observed power laws. Other studies have also found that SOC models do not reproduce the patterns of observed fires (McKenzie & Kennedy 2012). Thus a mechanism which resembles SOC, i.e. with a double separation of scales, does not seem a plausible explanation for the global forest dynamics.

The mechanism suggested by Pueyo et al. (2010) is isotropic percolation, when a system is near the critical point power law structures arise. This is equivalent to the random forest model that we explained previously, and requires the tuning of an external environmental condition to carry the system to this point. We did not expect forest growth to be a random process at local scales, but it is possible that combinations of factors cancel out to produce seemingly random forest dynamics at large scales. If this is the case the power law exponent should be theoretically near $\alpha = 2.055$, this is close but outside the confidence interval we observed (1.898 - 1.920), and thus other explanations are needed.

The third mechanism suggested as the cause of pervasive power laws in patch size distribution is facilitation (Manor & Shnerb 2008; Irvine, Bull & Keeling 2016): a patch surrounded by forest will have a smaller probability of been deforested or degraded than an isolated patch. We hypothesize that models that include facilitation could explain the patterns observed here. The model of Scanlon et al. (2007) represented the dynamics of savanna trees includes a global constraint (mean rainfall), a local facilitation mechanism, and two states (tree/non-tree), producing power laws across a rainfall gradient without the need for tuning an external parameter. The results for this model showed an $\alpha = 1.34$ which is also different from our results. Another model but with three states (tree/non-tree/degraded), including local facilitation and grazing, was also used to obtain power laws patch distributions without external tuning, and exhibited deviations from power laws at high grazing pressures (Kéfi et al. 2007). The values of the power law exponent α obtained for this model are dependent on the intensity of facilitation, when facilitation is more intense the exponent is higher, but the maximal values they obtained are still lower than the ones we observed. The interesting point is that the value of the exponent is dependent on the parameters, and thus the observed α might be obtained with some parameter combination. Kéfi et al. (2007) proposed that a deviation in power law behavior with the form of an exponential decay or cut-off could be a signal of a critical transition. At the continental scales studied here, we did not observe exponential cut-offs, but did observe other signals of a

346 transition. This confirms previous results (Weerman *et al.* 2012; Kéfi *et al.* 2014) showing that different
347 mechanisms can produce seemingly different spatial patterns near the transition, and that early warnings
348 based only on spatial patterns are not universal for all systems.

349 It has been suggested that a combination of spatial and temporal indicators could more reliably detect
350 critical transitions (Kéfi *et al.* 2014). In this study, we combined five criteria to detect the closeness to a
351 fragmentation threshold. Two of them were spatial: the forest patch size distribution, and the proportion
352 of the largest patch relative to total forest area (RS_{max}). The other three were the distribution of temporal
353 fluctuations in the largest patch size, the trend in the variance, and the skewness of the fluctuations. Each
354 one of these is not a strong individual predictor, but their combination gives us an increased degree of
355 confidence about the system being close to a critical transition.

356 We found that only the tropical forest of Africa and South America met all five criteria, and thus seem to
357 be near a critical fragmentation threshold. This confirms previous studies that point to this two tropical
358 areas as the most affected by deforestation (Hansen *et al.* 2013). Africa seems to be more affected, because
359 the proportion of the largest patch relative to total forest area (RS_{max}) is near 30%, which could indicate
360 that the transition is already started. Moreover, this region was estimated to be potentially bistable, with
361 the possibility to completely transform into a savanna (Staver, Archibald & Levin 2011). The main driver
362 of deforestation in this area was smallholder farming. The agro-industrial farming has been limited by the
363 growth of mineral and fossil-fuel sector, the lack of infrastructure, the political instability and the rural-urban
364 migrations (Rudel 2013). If these impediments can be surpassed a rapid growth of agro-industrial farming
365 could be produced with devastating consequences.

366 The region of South America tropical forest has a RS_{max} of more than 60% suggesting that the fragmentation
367 transition is approaching but not yet started. In this region, a striking decline in deforestation rates has
368 been observed in Brasil, which hosts most of the biggest forest patch, but deforestation rates have continued
369 to increase in surrounding countries (Argentina, Paraguay, Bolivia, Colombia, Peru) thus the region is still
370 at a high risk.

371 The monitoring of biggest patches is also important because they contain most of the intact forest landscapes
372 defined by Potapov *et al.* (2008), thus a relatively simple way to evaluate the risk in these areas is to use
373 RS_{max} index. The analysis of RS_{max} reveals that the island of Philippines (SEAS2) seems to be an example
374 of a critical transition from an unconnected to a connected state, the early warning signals can be qualitatively
375 observed: a big fluctuation in a negative direction precedes the transition and then RS_{max} stabilizes over
376 60% (Figure S9). Besides that there was a total loss of forest cover of 1.9% from year 2000 to 2012 (Hansen *et*
377 *al.* 2013) and deforestation rates were not substantially reduced in 1990-2014, this could be the results of an

378 active intervention of the government promoting conservation and rehabilitation of protected areas, ban of
379 logging old-growth forest, reforestation of barren areas, community-based forestry activities, and sustainable
380 forest management in the country's production forest (Lasco *et al.* 2008). This confirms that the early
381 warning indicators proposed here work in the correct direction.

382 The region of Southeast Asia was also in the first places of deforestation, but was not detected as a region
383 near a fragmentation threshold. This is probably due to the forest conservation and restoration programs
384 implemented by the Chinese government, which bans logging in natural forests and monitor illegal harvesting
385 (Viña *et al.* 2016). This is observed in the animations of largest patches (Appendix S3), the biggest patch
386 inside China connects to the biggest patch of surrounding countries and produce the positive fluctuations
387 of RS_{max} . Anyway, the MODIS dataset does not detect if native forest is replaced by agroindustrial tree
388 plantations like oil palms, that are among the main drivers of deforestation in this area (Malhi *et al.* 2014).
389 To improve the estimation of forest patches, data sets as the MODIS cropland probability and others about
390 land use, protected areas, forest type, should be incorporated (Hansen *et al.* 2014; Sexton *et al.* 2015).

391 Deforestation and fragmentation are closely related, at low levels of habitat reduction species population
392 will decline proportionally; this can happen even when the habitat fragments retain connectivity. As habi-
393 tat reduction continues, the critical threshold is approached and connectivity will have large fluctuations
394 (Brook *et al.* 2013). This could trigger several negative synergistic effects: populations fluctuations and the
395 possibility of extinctions will rise, increasing patch isolation and decreasing connectivity (Brook *et al.* 2013).

396 This positive feedback mechanism will be enhanced when the fragmentation threshold is reached, resulting
397 in the loss of most habitat specialist species at a landscape scale (Pardini *et al.* 2010). Some authors argue
398 that since species have heterogeneous responses to habitat loss and fragmentation, and biotic dispersal is
399 limited, the importance of thresholds is restricted to local scales or even that its existence is questionable
400 (Brook *et al.* 2013). Fragmentation is by definition a local process that at some point produces emergent
401 phenomena over the entire landscape, even if the area considered is infinite (Oborny, Meszéna & Szabó
402 2005). In addition, after a region's fragmentation threshold connectivity decreases, there is still a large and
403 internally well connected patch that can maintain sensitive species (Martensen *et al.* 2012). What is the
404 time needed for these large patches to become fragmented, and pose a real danger of extinction to a myriad
405 of sensitive species? If a forest is already in a fragmented state, a second critical transition from forest to
406 non-forest could happen, this was called the desertification transition (Corrado *et al.* 2014). Considering
407 the actual trends of habitat loss, and studying the dynamics of non-forest patches—instead of the forest
408 patches as we did here—the risk of this kind of transition could be estimated. The simple models proposed
409 previously could also be used to estimate if these thresholds are likely to be continuous and reversible or

discontinuous and often irreversible (Weissmann & Shnerb 2016), and the degree of protection (e.g. using the set-asides strategy Banks-Leite *et al.* (2014)) than would be necessary to stop this trend.

The effectiveness of landscape management is related to the degree of fragmentation, and the criteria to direct reforestation efforts could be focused on regions near a transition (Oborny *et al.* 2007). Regions that are in an unconnected state require large efforts to recover a connected state, but regions that are near a transition could be easily pushed to a connected state; feedbacks due to facilitation mechanisms might help to maintain this state. If the largest patch is always the same patch over time, the forest is probably not fragmented. This patch could represent a core area for conservation because it maintains the connectivity of the whole region. The dynamical fragmentation analysis that we did could be performed at smaller scales that would be more amenable to be managed for conservation, and their results could be readily applicable to modify the fragmentation of an area.

Crossing the fragmentation critical point in forests could have negative effects on biodiversity and ecosystem services (Haddad *et al.* 2015), but it could also produce feedback loops at different levels of the biological hierarchy. This means that a critical transition produced at a continental scale could have effects at the level of communities, food webs, populations, phenotypes and genotypes (Barnosky *et al.* 2012). All these effects interact with climate change, thus there is a potential production of cascading effects that could lead to a global collapse. Therefore, even if critical thresholds are reached only in some forest regions at a continental scale, a cascading effect with global consequences could still be produced, and may contribute to reach a planetary tipping point (Reyer *et al.* 2015). The risk of such event will be higher if the dynamics of separate continental regions are coupled (Lenton & Williams 2013). Using the time series obtained in this work the coupling of the continental could be further investigated. It has been proposed that to assess the probability of a global scale shift, different small scale ecosystems should be studied in parallel (Barnosky *et al.* 2012). As forest comprises a major proportion of such ecosystems, we think that the transition of forests could be used as a proxy for all the underling changes and as a successful predictor of a planetary tipping point.

Supporting information

- Appendix S1:** Supplementary data, Csv text file with model fits for patch size distribution, and model selection for all the regions.
- Appendix S2:** Gif Animations of a forest model percolation. These are animations showing the subcritical, critical, and super critical states.
- Appendix S3:** Gif Animations of largest patches. These show the temporal dynamics of the two largest

⁴⁴⁰ patches.

⁴⁴¹ **Appendix S4:** Tables and figures.

⁴⁴² *Table S1:* Proportion of Power law models not rejected by the goodness of fit test at $p \leq 0.05$ level.

⁴⁴³ *Table S2:* Generalized least squares fit by maximizing the restricted log-likelihood.

⁴⁴⁴ *Table S3:* Simultaneous Tests for General Linear Hypotheses of the power law exponent.

⁴⁴⁵ *Table S4:* Quantile regressions of the proportion of largest patch area vs year.

⁴⁴⁶ *Table S5:* Unbiased estimation of skewness for absolute largest patch fluctuations and relative fluctuations.

⁴⁴⁷ *Table S6:* Model selection using Akaike criterion for largest patch fluctuations in absolute values

⁴⁴⁸ *Table S7:* Model selection for fluctuation of largest patch in relative to total forest area.

⁴⁴⁹ *Figure S1:* Regions for Africa (AF), 1 Mainland, 2 Madagascar.

⁴⁵⁰ *Figure S2:* Regions for Eurasia (EUAS), 1 Mainland, 2 Japan, 3 United Kingdom.

⁴⁵¹ *Figure S3:* Regions for North America (NA), 1 Mainland, 5 Newfoundland.

⁴⁵² *Figure S4:* Regions for Australia and islands (OC), 1 Australia mainland; 2 New Guinea; 3 Malaysia/Kalimantan;

⁴⁵³ 4 Sumatra; 5 Sulawesi; 6 New Zealand south island; 7 Java; 8 New Zealand north island.

⁴⁵⁴ *Figure S5:* Regions for South America, SAST1 Tropical and subtropical forest up to Mexico; SAST2 Cuba;

⁴⁵⁵ SAT1 South America, Temperate forest.

⁴⁵⁶ *Figure S6:* Regions for Southeast Asia (SEAS), 1 Mainland; 2 Philippines.

⁴⁵⁷ *Figure S7:* Proportion of best models selected for patch size distributions using the Akaike criterion.

⁴⁵⁸ *Figure S8:* Power law exponents for forest patch distributions by year.

⁴⁵⁹ *Figure S9:* Largest patch proportion relative to total forest area RS_{max} , for regions with total forest area

⁴⁶⁰ less than 10^7 km^2 .

⁴⁶¹ *Figure S10:* Fluctuations of largest patch for regions with total forest area less than 10^7 km^2 . The patch

⁴⁶² sizes are relativized to the total forest area for that year.

⁴⁶³ **Data Accessibility**

⁴⁶⁴ The patch size files for all years and regions used here, and all the R and Matlab scripts are available at

⁴⁶⁵ figshare <http://dx.doi.org/10.6084/m9.figshare.4263905>.

466 **Acknowledgments**

467 LAS and SRD are grateful to the National University of General Sarmiento for financial support. This work
468 was partially supported by a grant from CONICET (PIO 144-20140100035-CO).

469 **References**

- 470 Allington, G.R.H. & Valone, T.J. (2010) Reversal of desertification: The role of physical and chemical soil
471 properties. *Journal of Arid Environments*, **74**, 973–977.
- 472 Banks-Leite, C., Pardini, R., Tambosi, L.R., Pearse, W.D., Bueno, A.A., Bruscagin, R.T., Condez, T.H.,
473 Dixo, M., Igari, A.T., Martensen, A.C. & Metzger, J.P. (2014) Using ecological thresholds to evaluate the
474 costs and benefits of set-asides in a biodiversity hotspot. *Science*, **345**, 1041–1045.
- 475 Barnosky, A.D., Hadly, E.A., Bascompte, J., Berlow, E.L., Brown, J.H., Fortelius, M., Getz, W.M., Harte, J.,
476 Hastings, A., Marquet, P.A., Martinez, N.D., Mooers, A., Roopnarine, P., Vermeij, G., Williams, J.W., Gille-
477 spie, R., Kitzes, J., Marshall, C., Matzke, N., Mindell, D.P., Revilla, E. & Smith, A.B. (2012) Approaching
478 a state shift in Earth’s biosphere. *Nature*, **486**, 52–58.
- 479 Bascompte, J. & Solé, R.V. (1996) Habitat fragmentation and extinction thresholds in spatially explicit
480 models. *Journal of Animal Ecology*, **65**, 465–473.
- 481 Bazant, M.Z. (2000) Largest cluster in subcritical percolation. *Physical Review E*, **62**, 1660–1669.
- 482 Belward, A.S. (1996) *The IGBP-DIS Global 1 Km Land Cover Data Set “DISCover”: Proposal and Imple-
483 mentation Plans : Report of the Land Recover Working Group of IGBP-DIS*. IGBP-DIS Office.
- 484 Benedetti-Cecchi, L., Tamburello, L., Maggi, E. & Bulleri, F. (2015) Experimental Perturbations Modify the
485 Performance of Early Warning Indicators of Regime Shift. *Current biology*, **25**, 1867–1872.
- 486 Bestelmeyer, B.T., Ellison, A.M., Fraser, W.R., Gorman, K.B., Holbrook, S.J., Laney, C.M., Ohman, M.D.,
487 Peters, D.P.C., Pillsbury, F.C., Rassweiler, A., Schmitt, R.J. & Sharma, S. (2011) Analysis of abrupt tran-
488 sitions in ecological systems. *Ecosphere*, **2**, 129.
- 489 Boettiger, C. & Hastings, A. (2012) Quantifying limits to detection of early warning for critical transitions.
490 *Journal of The Royal Society Interface*, **9**, 2527–2539.
- 491 Bonan, G.B. (2008) Forests and Climate Change: Forcings, Feedbacks, and the Climate Benefits of Forests.
492 *Science*, **320**, 1444–1449.
- 493 Botet, R. & Ploszajczak, M. (2004) Correlations in Finite Systems and Their Universal Scaling Properties.

- 494 *Nonequilibrium physics at short time scales: Formation of correlations* (ed K. Morawetz), pp. 445–466.
495 Springer-Verlag, Berlin Heidelberg.
- 496 Brook, B.W., Ellis, E.C., Perring, M.P., Mackay, A.W. & Blomqvist, L. (2013) Does the terrestrial biosphere
497 have planetary tipping points? *Trends in Ecology & Evolution*.
- 498 Burnham, K. & Anderson, D.R. (2002) *Model selection and multi-model inference: A practical information-*
499 *theoretic approach*, 2nd. ed. Springer-Verlag, New York.
- 500 Canfield, D.E., Glazer, A.N. & Falkowski, P.G. (2010) The Evolution and Future of Earth's Nitrogen Cycle.
501 *Science*, **330**, 192–196.
- 502 Carpenter, S.R., Cole, J.J., Pace, M.L., Batt, R., Brock, W.A., Cline, T., Coloso, J., Hodgson, J.R., Kitchell,
503 J.F., Seekell, D.A., Smith, L. & Weidel, B. (2011) Early Warnings of Regime Shifts: A Whole-Ecosystem
504 Experiment. *Science*, **332**, 1079–1082.
- 505 Clauset, A., Shalizi, C. & Newman, M. (2009) Power-Law Distributions in Empirical Data. *SIAM Review*,
506 **51**, 661–703.
- 507 Corrado, R., Cherubini, A.M. & Pennetta, C. (2014) Early warning signals of desertification transitions in
508 semiarid ecosystems. *Physical Review E - Statistical, Nonlinear, and Soft Matter Physics*, **90**, 62705.
- 509 Crowther, T.W., Glick, H.B., Covey, K.R., Bettigole, C., Maynard, D.S., Thomas, S.M., Smith, J.R., Hintler,
510 G., Duguid, M.C., Amatulli, G., Tuanmu, M.-N., Jetz, W., Salas, C., Stam, C., Piotto, D., Tavani, R., Green,
511 S., Bruce, G., Williams, S.J., Wiser, S.K., Huber, M.O., Hengeveld, G.M., Nabuurs, G.-J., Tikhonova, E.,
512 Borchardt, P., Li, C.-F., Powrie, L.W., Fischer, M., Hemp, A., Homeier, J., Cho, P., Vibrans, A.C., Umunay,
513 P.M., Piao, S.L., Rowe, C.W., Ashton, M.S., Crane, P.R. & Bradford, M.A. (2015) Mapping tree density at
514 a global scale. *Nature*, **525**, 201–205.
- 515 Dai, L., Vorselen, D., Korolev, K.S. & Gore, J. (2012) Generic Indicators for Loss of Resilience Before a
516 Tipping Point Leading to Population Collapse. *Science*, **336**, 1175–1177.
- 517 DiMiceli, C., Carroll, M., Sohlberg, R., Huang, C., Hansen, M. & Townshend, J. (2015) Annual Global
518 Automated MODIS Vegetation Continuous Fields (MOD44B) at 250 m Spatial Resolution for Data Years
519 Beginning Day 65, 2000 - 2014, Collection 051 Percent Tree Cover, University of Maryland, College Park,
520 MD, USA.
- 521 Drake, J.M. & Griffen, B.D. (2010) Early warning signals of extinction in deteriorating environments. *Nature*,

- 522 **467**, 456–459.
- 523 Efron, B. & Tibshirani, R.J. (1994) *An Introduction to the Bootstrap*. Taylor & Francis, New York.
- 524 Filotas, E., Parrott, L., Burton, P.J., Chazdon, R.L., Coates, K.D., Coll, L., Haeussler, S., Martin, K.,
- 525 Nocentini, S., Puettmann, K.J., Putz, F.E., Simard, S.W. & Messier, C. (2014) Viewing forests through the
- 526 lens of complex systems science. *Ecosphere*, **5**, 1–23.
- 527 Foley, J.A., Ramankutty, N., Brauman, K.A., Cassidy, E.S., Gerber, J.S., Johnston, M., Mueller, N.D.,
- 528 O'Connell, C., Ray, D.K., West, P.C., Balzer, C., Bennett, E.M., Carpenter, S.R., Hill, J., Monfreda, C.,
- 529 Polasky, S., Rockström, J., Sheehan, J., Siebert, S., Tilman, D. & Zaks, D.P.M. (2011) Solutions for a
- 530 cultivated planet. *Nature*, **478**, 337–342.
- 531 Folke, C., Jansson, Å., Rockström, J., Olsson, P., Carpenter, S.R., Iii, F.S.C., Crépin, A.-S., Daily, G.,
- 532 Danell, K., Ebbesson, J., Elmquist, T., Galaz, V., Moberg, F., Nilsson, M., Österblom, H., Ostrom, E.,
- 533 Persson, Å., Peterson, G., Polasky, S., Steffen, W., Walker, B. & Westley, F. (2011) Reconnecting to the
- 534 Biosphere. *AMBIO*, **40**, 719–738.
- 535 Fung, T., O'Dwyer, J.P., Rahman, K.A., Fletcher, C.D. & Chisholm, R.A. (2016) Reproducing static and
- 536 dynamic biodiversity patterns in tropical forests: the critical role of environmental variance. *Ecology*, **97**,
- 537 1207–1217.
- 538 Gardner, R.H. & Urban, D.L. (2007) Neutral models for testing landscape hypotheses. *Landscape Ecology*,
- 539 **22**, 15–29.
- 540 Gastner, M.T., Oborny, B., Zimmermann, D.K. & Pruessner, G. (2009) Transition from Connected to Frag-
- 541 mented Vegetation across an Environmental Gradient: Scaling Laws in Ecotone Geometry. *The American*
- 542 *Naturalist*, **174**, E23–E39.
- 543 Gillespie, C.S. (2015) Fitting Heavy Tailed Distributions: The poweRlaw Package. *Journal of Statistical*
- 544 *Software*, **64**, 1–16.
- 545 Gilman, S.E., Urban, M.C., Tewksbury, J., Gilchrist, G.W. & Holt, R.D. (2010) A framework for community
- 546 interactions under climate change. *Trends in Ecology & Evolution*, **25**, 325–331.
- 547 Goldstein, M.L., Morris, S.A. & Yen, G.G. (2004) Problems with fitting to the power-law distribution. *The*
- 548 *European Physical Journal B - Condensed Matter and Complex Systems*, **41**, 255–258.
- 549 Haddad, N.M., Brudvig, L.a., Clobert, J., Davies, K.F., Gonzalez, A., Holt, R.D., Lovejoy, T.E., Sexton,
- 550 J.O., Austin, M.P., Collins, C.D., Cook, W.M., Damschen, E.I., Ewers, R.M., Foster, B.L., Jenkins, C.N.,
- 551 King, a.J., Laurance, W.F., Levey, D.J., Margules, C.R., Melbourne, B.a., Nicholls, a.O., Orrock, J.L.,

- 552 Song, D.-X. & Townshend, J.R. (2015) Habitat fragmentation and its lasting impact on Earth's ecosystems.
- 553 *Science Advances*, **1**, 1–9.
- 554 Hansen, M., Potapov, P., Margono, B., Stehman, S., Turubanova, S. & Tyukavina, A. (2014) Response to
- 555 Comment on “High-resolution global maps of 21st-century forest cover change”. *Science*, **344**, 981.
- 556 Hansen, M.C., Potapov, P.V., Moore, R., Hancher, M., Turubanova, S.A., Tyukavina, A., Thau, D., Stehman,
- 557 S.V., Goetz, S.J., Loveland, T.R., Kommareddy, A., Egorov, A., Chini, L., Justice, C.O. & Townshend, J.R.G.
- 558 (2013) High-Resolution Global Maps of 21st-Century Forest Cover Change. *Science*, **342**, 850–853.
- 559 Hantson, S., Pueyo, S. & Chuvieco, E. (2015) Global fire size distribution is driven by human impact and
- 560 climate. *Global Ecology and Biogeography*, **24**, 77–86.
- 561 Harris, T.E. (1974) Contact interactions on a lattice. *The Annals of Probability*, **2**, 969–988.
- 562 Hastings, A. & Wysham, D.B. (2010) Regime shifts in ecological systems can occur with no warning. *Ecology*
- 563 *Letters*, **13**, 464–472.
- 564 He, F. & Hubbell, S. (2003) Percolation Theory for the Distribution and Abundance of Species. *Physical*
- 565 *Review Letters*, **91**, 198103.
- 566 Hinrichsen, H. (2000) Non-equilibrium critical phenomena and phase transitions into absorbing states. *Ad-*
- 567 *vances in Physics*, **49**, 815–958.
- 568 Irvine, M.A., Bull, J.C. & Keeling, M.J. (2016) Aggregation dynamics explain vegetation patch-size distri-
- 569 *butions*. *Theoretical Population Biology*, **108**, 70–74.
- 570 Keitt, T.H., Urban, D.L. & Milne, B.T. (1997) Detecting critical scales in fragmented landscapes. *Conser-*
- 571 *vation Ecology*, **1**, 4.
- 572 Kéfi, S., Guttal, V., Brock, W.A., Carpenter, S.R., Ellison, A.M., Livina, V.N., Seekell, D.A., Scheffer, M.,
- 573 Nes, E.H. van & Dakos, V. (2014) Early Warning Signals of Ecological Transitions: Methods for Spatial
- 574 Patterns. *PLoS ONE*, **9**, e92097.
- 575 Kéfi, S., Rietkerk, M., Alados, C.L., Pueyo, Y., Papanastasis, V.P., ElAich, A. & Ruiter, P.C. de. (2007)
- 576 Spatial vegetation patterns and imminent desertification in Mediterranean arid ecosystems. *Nature*, **449**,
- 577 213–217.
- 578 Kitzberger, T., Aráoz, E., Gowda, J.H., Mermoz, M. & Morales, J.M. (2012) Decreases in Fire Spread Prob-
- 579 ability with Forest Age Promotes Alternative Community States, Reduced Resilience to Climate Variability

- 580 and Large Fire Regime Shifts. *Ecosystems*, **15**, 97–112.
- 581 Klaus, A., Yu, S. & Plenz, D. (2011) Statistical analyses support power law distributions found in neuronal
582 avalanches. (ed M Zochowski). *PloS one*, **6**, e19779.
- 583 Koenker, R. (2016) quantreg: Quantile Regression.
- 584 Lasco, R.D., Pulhin, F.B., Cruz, R.V.O., Pulhin, J.M., Roy, S.S.N. & Sanchez, P.A.J. (2008) Forest responses
585 to changing rainfall in the Philippines. *Climate change and vulnerability* (eds N. Leary, C. Conde & J.
586 Kulkarni), pp. 49–66. Earthscan, London.
- 587 Leibold, M.A. & Norberg, J. (2004) Biodiversity in metacommunities: Plankton as complex adaptive sys-
588 tems? *Limnology and Oceanography*, **49**, 1278–1289.
- 589 Lenton, T.M. & Williams, H.T.P. (2013) On the origin of planetary-scale tipping points. *Trends in Ecology
590 & Evolution*, **28**, 380–382.
- 591 Loehle, C., Li, B.-L. & Sundell, R.C. (1996) Forest spread and phase transitions at forest-prairie ecotones in
592 Kansas, U.S.A. *Landscape Ecology*, **11**, 225–235.
- 593 Malhi, Y., Gardner, T.A., Goldsmith, G.R., Silman, M.R. & Zelazowski, P. (2014) Tropical Forests in the
594 Anthropocene. *Annual Review of Environment and Resources*, **39**, 125–159.
- 595 Manor, A. & Shnerb, N.M. (2008) Origin of pareto-like spatial distributions in ecosystems. *Physical Review
596 Letters*, **101**, 268104.
- 597 Martensen, A.C., Ribeiro, M.C., Banks-Leite, C., Prado, P.I. & Metzger, J.P. (2012) Associations of Forest
598 Cover, Fragment Area, and Connectivity with Neotropical Understory Bird Species Richness and Abundance.
599 *Conservation Biology*, **26**, 1100–1111.
- 600 Martín, P.V., Bonachela, J.A., Levin, S.A. & Muñoz, M.A. (2015) Eluding catastrophic shifts. *Proceedings
601 of the National Academy of Sciences*, **112**, E1828–E1836.
- 602 McKenzie, D. & Kennedy, M.C. (2012) Power laws reveal phase transitions in landscape controls of fire
603 regimes. *Nat Commun*, **3**, 726.
- 604 Mitchell, M.G.E., Suarez-Castro, A.F., Martinez-Harms, M., Maron, M., McAlpine, C., Gaston, K.J., Jo-
605 hansen, K. & Rhodes, J.R. (2015) Reframing landscape fragmentation's effects on ecosystem services. *Trends
606 in Ecology & Evolution*, **30**, 190–198.
- 607 Naito, A.T. & Cairns, D.M. (2015) Patterns of shrub expansion in Alaskan arctic river corridors suggest

- 608 phase transition. *Ecology and Evolution*, **5**, 87–101.
- 609 Oborny, B., Meszéna, G. & Szabó, G. (2005) Dynamics of Populations on the Verge of Extinction. *Oikos*,
610 **109**, 291–296.
- 611 Oborny, B., Szabó, G. & Meszéna, G. (2007) Survival of species in patchy landscapes: percolation in space
612 and time. *Scaling biodiversity*, pp. 409–440. Cambridge University Press.
- 613 Ochoa-Quintero, J.M., Gardner, T.A., Rosa, I., de Barros Ferraz, S.F. & Sutherland, W.J. (2015) Thresholds
614 of species loss in Amazonian deforestation frontier landscapes. *Conservation Biology*, **29**, 440–451.
- 615 Ódor, G. (2004) Universality classes in nonequilibrium lattice systems. *Reviews of Modern Physics*, **76**,
616 663–724.
- 617 Pardini, R., Bueno, A. de A., Gardner, T.A., Prado, P.I. & Metzger, J.P. (2010) Beyond the Fragmentation
618 Threshold Hypothesis: Regime Shifts in Biodiversity Across Fragmented Landscapes. *PLoS ONE*, **5**, e13666.
- 619 Pinheiro, J., Bates, D., DebRoy, S., Sarkar, D. & R Core Team. (2016) *nlme: Linear and Nonlinear Mixed
620 Effects Models*.
- 621 Potapov, P., Yaroshenko, A., Turubanova, S., Dubinin, M., Laestadius, L., Thies, C., Aksenov, D., Egorov,
622 A., Yesipova, Y., Glushkov, I., Karpachevskiy, M., Kostikova, A., Manisha, A., Tsybikova, E. & Zhuravleva,
623 I. (2008) Mapping the world's intact forest landscapes by remote sensing. *Ecology and Society*, **13**.
- 624 Pueyo, S., de Alencastro Graça, P.M.L., Barbosa, R.I., Cots, R., Cardona, E. & Fearnside, P.M. (2010)
625 Testing for criticality in ecosystem dynamics: the case of Amazonian rainforest and savanna fire. *Ecology
626 Letters*, **13**, 793–802.
- 627 R Core Team. (2015) R: A Language and Environment for Statistical Computing.
- 628 Reyer, C.P.O., Rammig, A., Brouwers, N. & Langerwisch, F. (2015) Forest resilience, tipping points and
629 global change processes. *Journal of Ecology*, **103**, 1–4.
- 630 Rockstrom, J., Steffen, W., Noone, K., Persson, A., Chapin, F.S., Lambin, E.F., Lenton, T.M., Scheffer, M.,
631 Folke, C., Schellnhuber, H.J., Nykvist, B., Wit, C.A. de, Hughes, T., Leeuw, S. van der, Rodhe, H., Sorlin,
632 S., Snyder, P.K., Costanza, R., Svedin, U., Falkenmark, M., Karlberg, L., Corell, R.W., Fabry, V.J., Hansen,
633 J., Walker, B., Liverman, D., Richardson, K., Crutzen, P. & Foley, J.A. (2009) A safe operating space for
634 humanity. *Nature*, **461**, 472–475.
- 635 Rooij, M.M.J.W. van, Nash, B., Rajaraman, S. & Holden, J.G. (2013) A Fractal Approach to Dynamic

- 636 Inference and Distribution Analysis. *Frontiers in Physiology*, **4**.
- 637 Rudel, T.K. (2013) The national determinants of deforestation in sub-Saharan Africa. *Philosophical Trans-*
 638 *actions of the Royal Society B: Biological Sciences*, **368**, 20120405.
- 639 Saravia, L.A. & Momo, F.R. (2017) Biodiversity collapse and early warning indicators in a spatial phase
 640 transition between neutral and niche communities. *PeerJ PrePrints*, **5**, e1589v4.
- 641 Scanlon, T.M., Caylor, K.K., Levin, S.A. & Rodriguez-iturbe, I. (2007) Positive feedbacks promote power-law
 642 clustering of Kalahari vegetation. *Nature*, **449**, 209–212.
- 643 Scheffer, M., Bascompte, J., Brock, W.A., Brovkin, V., Carpenter, S.R., Dakos, V., Held, H., Nes, E.H.V.,
 644 Rietkerk, M. & Sugihara, G. (2009) Early-warning signals for critical transitions. *Nature*, **461**, 53–59.
- 645 Scheffer, M., Walker, B., Carpenter, S., Foley, J. a, Folke, C. & Walker, B. (2001) Catastrophic shifts in
 646 ecosystems. *Nature*, **413**, 591–596.
- 647 Seidler, T.G. & Plotkin, J.B. (2006) Seed Dispersal and Spatial Pattern in Tropical Trees. *PLoS Biology*, **4**,
 648 e344.
- 649 Sexton, J.O., Noojipady, P., Song, X.-P., Feng, M., Song, D.-X., Kim, D.-H., Anand, A., Huang, C., Channan,
 650 S., Pimm, S.L. & Townshend, J.R. (2015) Conservation policy and the measurement of forests. *Nature*
 651 *Climate Change*, **6**, 192–196.
- 652 Sole, R.V., Alonso, D. & Mckane, A. (2002) Self-organized instability in complex ecosystems. *Philosophical*
 653 *transactions of the Royal Society of London. Series B, Biological sciences*, **357**, 667–681.
- 654 Solé, R.V. (2011) *Phase Transitions*. Princeton University Press.
- 655 Solé, R.V. & Bascompte, J. (2006) *Self-organization in complex ecosystems*. Princeton University Press, New
 656 Jersey, USA.
- 657 Solé, R.V., Alonso, D. & Saldaña, J. (2004) Habitat fragmentation and biodiversity collapse in neutral
 658 communities. *Ecological Complexity*, **1**, 65–75.
- 659 Solé, R.V., Bartumeus, F. & Gamarra, J.G.P. (2005) Gap percolation in rainforests. *Oikos*, **110**, 177–185.
- 660 Stauffer, D. & Aharony, A. (1994) *Introduction To Percolation Theory*. Taylor & Francis, London.
- 661 Staver, A.C., Archibald, S. & Levin, S.A. (2011) The Global Extent and Determinants of Savanna and Forest
 662 as Alternative Biome States. *Science*, **334**, 230–232.
- 663 Vasilakopoulos, P. & Marshall, C.T. (2015) Resilience and tipping points of an exploited fish population over

- 664 six decades. *Global Change Biology*, **21**, 1834–1847.
- 665 Viña, A., McConnell, W.J., Yang, H., Xu, Z. & Liu, J. (2016) Effects of conservation policy on China's forest
666 recovery. *Science Advances*, **2**, e1500965.
- 667 Weerman, E.J., Van Belzen, J., Rietkerk, M., Temmerman, S., Kéfi, S., Herman, P.M.J. & Koppell, J.V.
668 de. (2012) Changes in diatom patch-size distribution and degradation in a spatially self-organized intertidal
669 mudflat ecosystem. *Ecology*, **93**, 608–618.
- 670 Weissmann, H. & Shnerb, N.M. (2016) Predicting catastrophic shifts. *Journal of Theoretical Biology*, **397**,
671 128–134.
- 672 Zhang, J.Y., Wang, Y., Zhao, X., Xie, G. & Zhang, T. (2005) Grassland recovery by protection from grazing
673 in a semi-arid sandy region of northern China. *New Zealand Journal of Agricultural Research*, **48**, 277–284.
- 674 Zinck, R.D. & Grimm, V. (2009) Unifying wildfire models from ecology and statistical physics. *The American
675 naturalist*, **174**, E170–85.
- 676 Zuur, A.F., Ieno, E.N., Walker, N., Saveliev, A.A. & Smith, G.M. (2009) *Mixed effects models and extensions
677 in ecology with R*. Springer New York, New York, NY.